

## Supplementary Information

### **Bioinspired hydrogel microfibres colour-encoded with colloidal crystals**

*Zhi-Jun Meng, Jing Zhang, Xu Deng, Ji Liu, Ziyi Yu, and Chris Abell*

#### **Part I. Supplementary Experimental Details**

#### **Part II. Supplementary Figures**

#### **Part III. Supplementary Videos**

## **Part I. Supplementary Experimental Details**

### **Chemicals and Materials**

All chemicals were of analytical grade and used without further purification. Trimethylolpropane ethoxylate triacrylate ( $M_n \sim 428$ , ETPTA), alginic acid sodium salt from brown algae (low viscosity) and 2-Hydroxy-2-methyl-propiofenone (97%, 1173) were purchased from Sigma–Aldrich. Ethanol absolute was purchased from VWR, UK. Milli-Q water with resistance greater than  $18 \text{ M}\Omega \cdot \text{cm}^{-1}$  was used for the preparation of all aqueous solutions.

### **Preparation of Colloidal Crystal Suspensions**

Monodispersed  $\text{SiO}_2$  colloids were synthesized through a sol-gel process by the modified Stöber method.<sup>1</sup> An ethanolic suspension of the  $\text{SiO}_2$  particles was mixed with an ETPTA containing 2 wt% photoinitiator 1173. After complete mixing, the mixture was left in an oven at  $60 \text{ }^\circ\text{C}$  for 24 h to completely remove the ethanol. The quantities of  $\text{SiO}_2$  colloids and ETPTA were chosen such that the weight fraction of colloids in ETPTA in the ethanol-free base was 25% (w/w).

### **Microfluidic Device Fabrication**

The coaxial microcapillary microfluidic devices were fabricated by following the previous protocol.<sup>2</sup> Briefly, an injection capillary was inserted into one end of square capillary (CM Scientific Ltd, UK) with an inner width of 1 mm. These two capillaries were axially centered on a microscope slide and fixed in a position using two-part epoxy glue (5-Minute Epoxy® Devcon). The collection capillary was then inserted into the square capillary, placed at a desirable distance from the injection capillary, axially centered and fix to the microscope slide. Dispensing needles were placed at the intersections of the injection and collection capillary with the square capillary, which were used to introduce the oil and water phase.

### **Characterizations**

The colour-encoded microfibre generation progress was monitored and recorded using a Vision Research Phantom Miro ex4-M fast camera, attached to an Olympus IX71 inverted microscope. The bright field images were taken by the fast camera and the optical images of the encoding microfibres were taken by the Leica Stereo microscope. The spectra of colloidal

crystals were read by a fibre optic spectrometer (Ocean Optics, USB4000), attached to an Olympus IX71 inverted microscope. Scanning electron microscopy (SEM) measurements of the microfibrils and the colloidal crystals were made by using a Leo 1530 variable pressure SEM with InLens detector.

## References

1. W. Stober, A. Fink and E. Bohn, *Colloid Interface Sci.*, 1968, **26**, 62-69.
2. Z. J. Meng, W. Wang, R. Xie, X. J. Ju, Z. Liu and L. Y. Chu, *Lab on a chip*, 2016, **16**, 2673-2681.

## Part II. Supplementary Figures

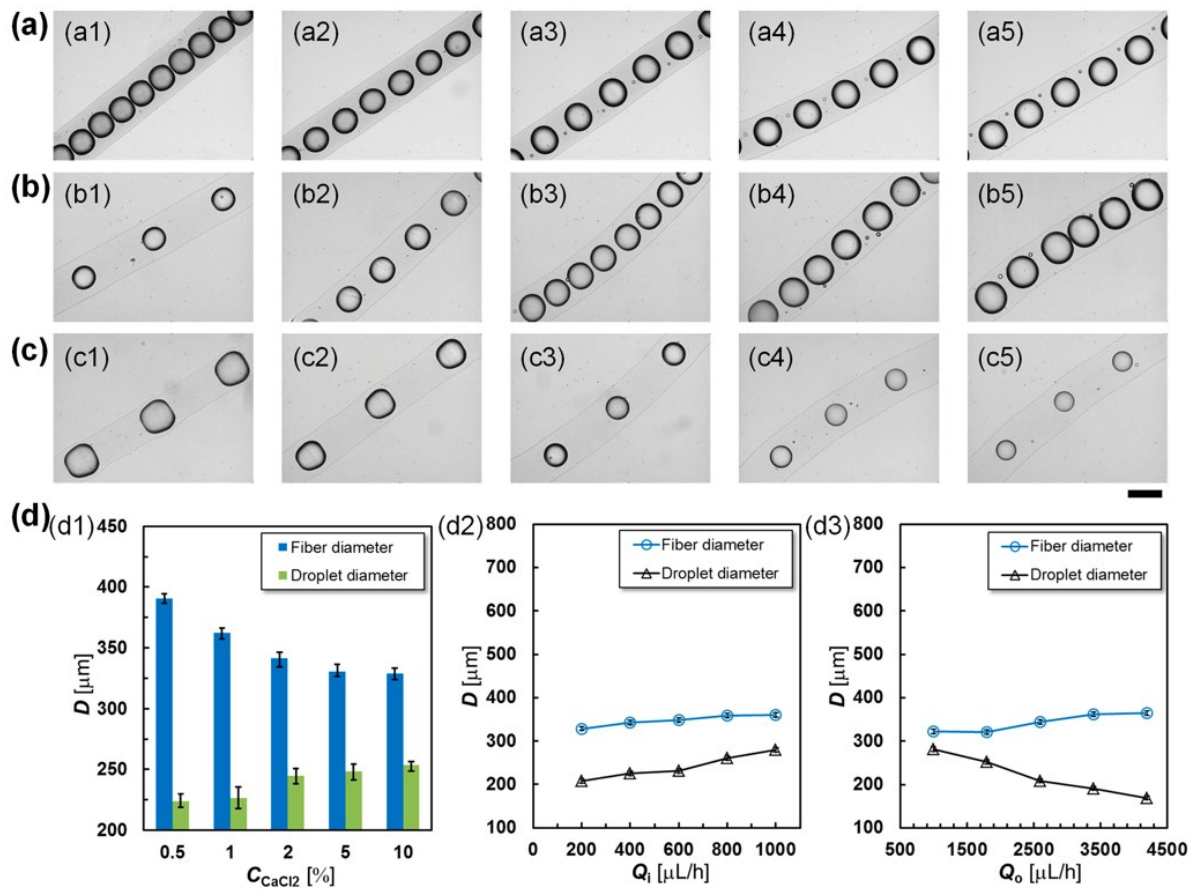


**Figure S1.** Variation in the diameters of fibres and diameters of droplets as a function of concentration of CaCl<sub>2</sub>, the flow rate of inter oil phase ( $Q_i$ ), and the flow rate of outer aqueous phase ( $Q_o$ ). The scale bar in Figures a-c is 300 μm. (a, d1) Concentration of CaCl<sub>2</sub>-dependence of diameters of the fibre and the droplet. The flow rates  $Q_i$  and  $Q_o$  were at 300 μL.h<sup>-1</sup> and 2000 μL.h<sup>-1</sup>. The concentration of CaCl<sub>2</sub> in the reservoir was at 0.5% (a1), 1% (a2), 2% (a3), 5% (a4) and 10% (a5), respectively. (b, d2) Flow rate of  $Q_i$ -dependence of diameters of the fibre and diameters of the droplet. The flow rate  $Q_o$  was at 3000 μL.h<sup>-1</sup>, the flow rate  $Q_i$  was at 200 (b1), 400 (b2), 600 (b3), 800 (b4) and 1000 μL.h<sup>-1</sup> (b5), respectively. (c, d3) Flow rate of  $Q_o$ -dependence of diameters of the fibre and diameters of the droplet. The flow rate  $Q_i$  was at 200 μL.h<sup>-1</sup>, the  $Q_o$  was at 1000 (c1), 1800 (c2), 2600 (c3), 3400 (c4) and 4200 μL.h<sup>-1</sup> (c5), respectively. The diameter of Ca-alginate microfibres decreases with the increasing the concentration of the CaCl<sub>2</sub> (d1); The diameter of both Ca-alginate microfibres and the incorporated microdroplets increases with the increasing the flow rate  $Q_i$  (d2); The diameter of Ca-alginate microfibres increases with the increasing the flow rate  $Q_o$ , while that of the diameter of incorporated microdroplets decreases with the increasing the flow rate  $Q_o$  (d3).

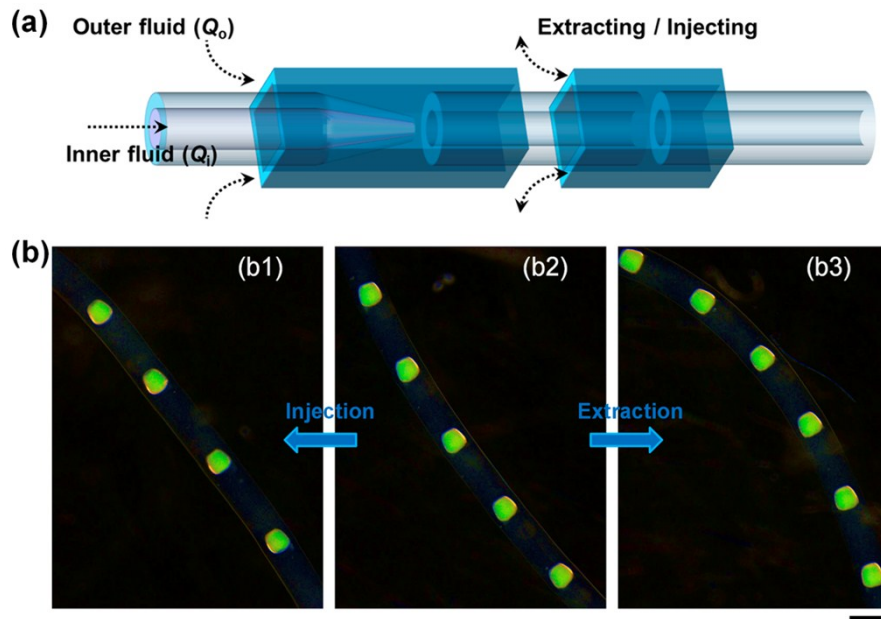


**Figure S2.** Microfluidic fabrication of colour-encoded microfibres with tuneable distance of the encapsulated colloidal crystal dots. (a) Schematic diagram of the microfluidic device. In this method, we kept the flow rate of  $Q_i$  and  $Q_o$  constant during the droplets formation process, and then either the alginate solution was extracted from the microfluidic device, or the additional alginate solution was injected to the microfluidic device. (b) Optical micrographs of the colour encoded-microfibres with tuneable interval distance between the colloidal crystal dots. The flow rates  $Q_i$  and  $Q_o$  were at 200 and 3000  $\mu\text{L}\cdot\text{h}^{-1}$ , individually. The flow rates of injection and extraction of the alginate solution were both at 1000  $\mu\text{L}\cdot\text{h}^{-1}$ . The interval distance between the colloidal crystal dots in the microfibre increases when an additional alginate solution is injected into the device (b1). The distance decreases when the alginate solution is extracted from the device (b2). The scale bar is 500  $\mu\text{m}$ .

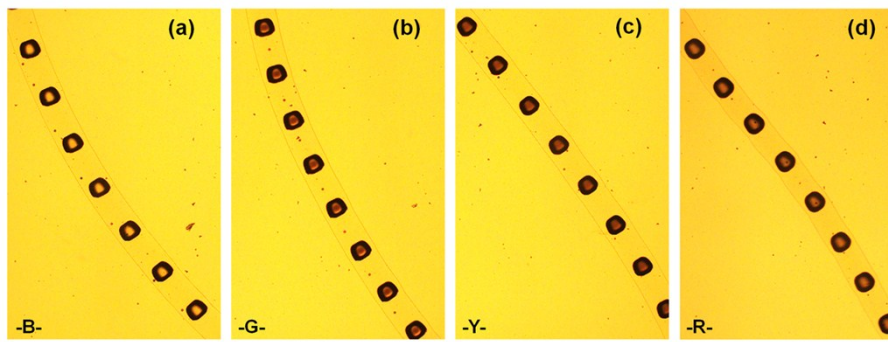


**Figure S3.** Optical microscope images of the colour-encoded microfibres with one type of colloidal crystal microdot under transmission mode. The scale bar is 500  $\mu\text{m}$ .

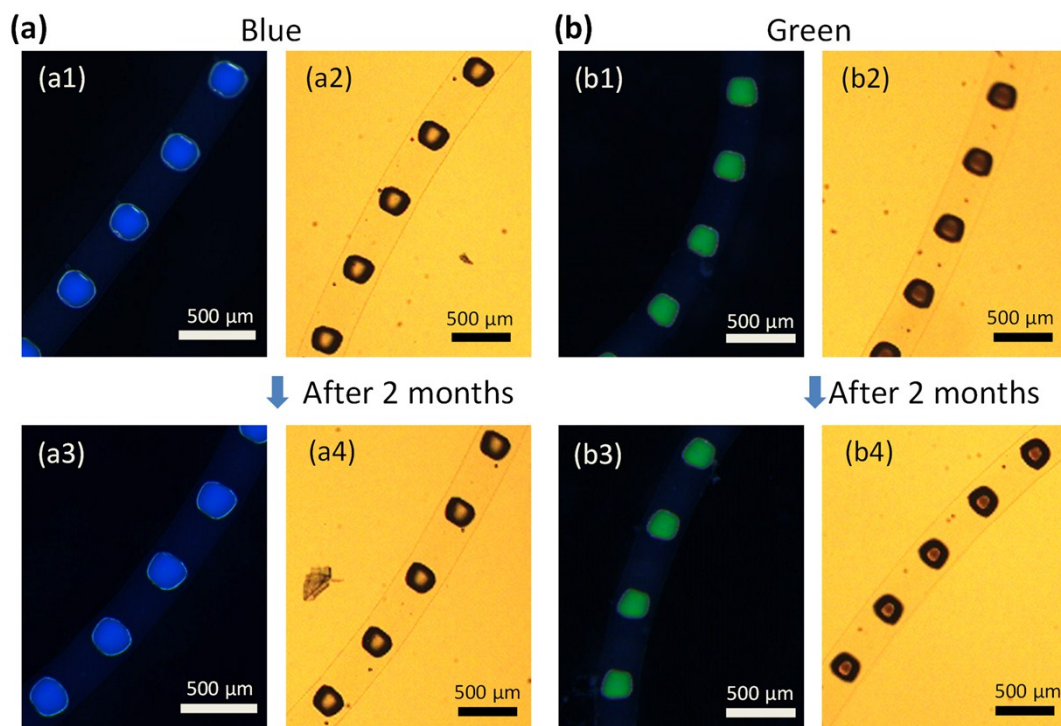


**Figure S4.** Photographs demonstration of the stability of the colour-encoded microfibres and the non-fading behavior of the colloidal crystal microdots. The obtained microfibres were kept in an aqueous solution containing  $\text{Ca}^{2+}$  (0.3 % w/v) for two months. Optical images of the microfibres were recorded at the beginning and the end. As shown in the images, all the colloidal crystal microdots still remain their original bright structure colours of blue (a1, a3) and green (b1, b3). Meanwhile, the colour-encoded microfibres remain the geometry and transparency property within the months (a2, a4, b2, b4). All above demonstrate the good time-dependent stability of the colour-encoded microfibres.

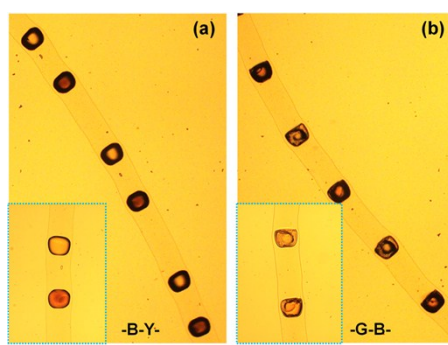


**Figure S5.** Optical microscope images of the colour-encoded microfibres with two different types of colloidal crystal microdots under transmission mode. (a) Microfibre encoded with “-B-Y-” colloidal crystal microdots. (b) Microfibre encoded with “-G-B-” colloidal crystal microdots. The scale bar is 500  $\mu\text{m}$ .

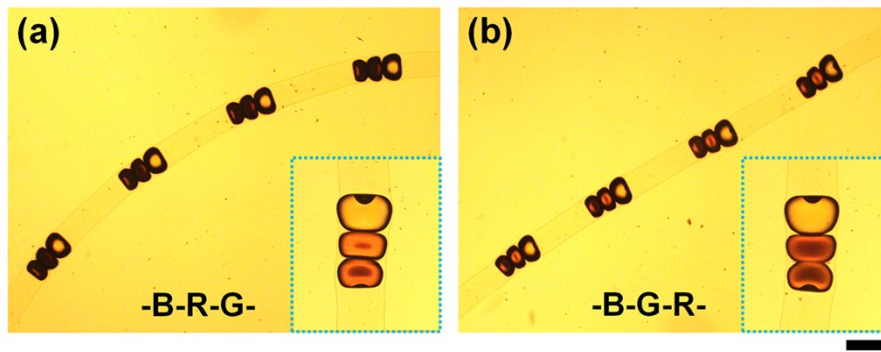


**Figure S6.** Optical microscope images of the colour-encoded microfibres with three different types of colloidal crystal microdots under transmission mode. (a) Microfibre with the encoding unit pattern “-B-R-G-”. (b) Microfibre with the encoding unit pattern “-B-G-R-”. The scale bar is 500  $\mu\text{m}$ .

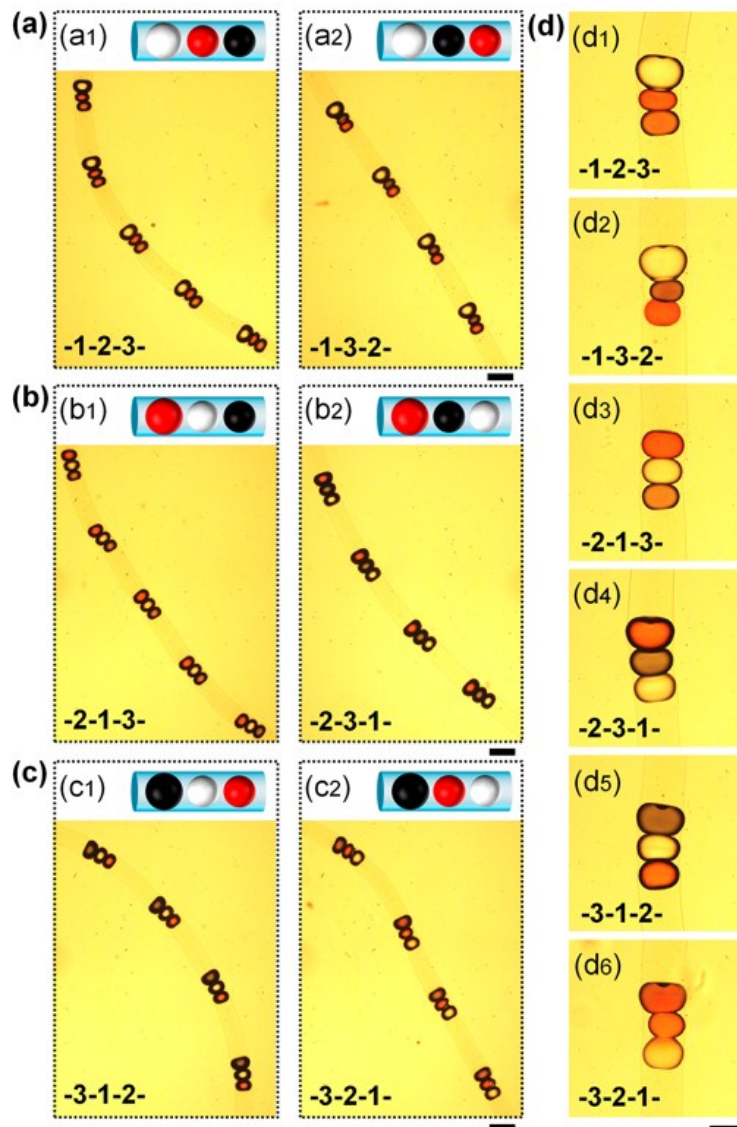


**Figure S7.** Schematics and optical microscope images (a-c) of the encoded microfibres with three different microdots. (a) Microfibre with the encoding unit pattern “-1-2-3-” and “-1-3-2-”. (b) Microfibre with the encoding unit pattern “-2-1-3-” and “-2-3-1-”. (c) Microfibres with the encoding unit pattern “-1-2-3-” and “-1-3-2-”. (d) Magnified optical microscope images of the encoding unit of the microfibres. Scale bars are 500  $\mu\text{m}$  for (a), (b) and (c), and 300  $\mu\text{m}$  for (d).

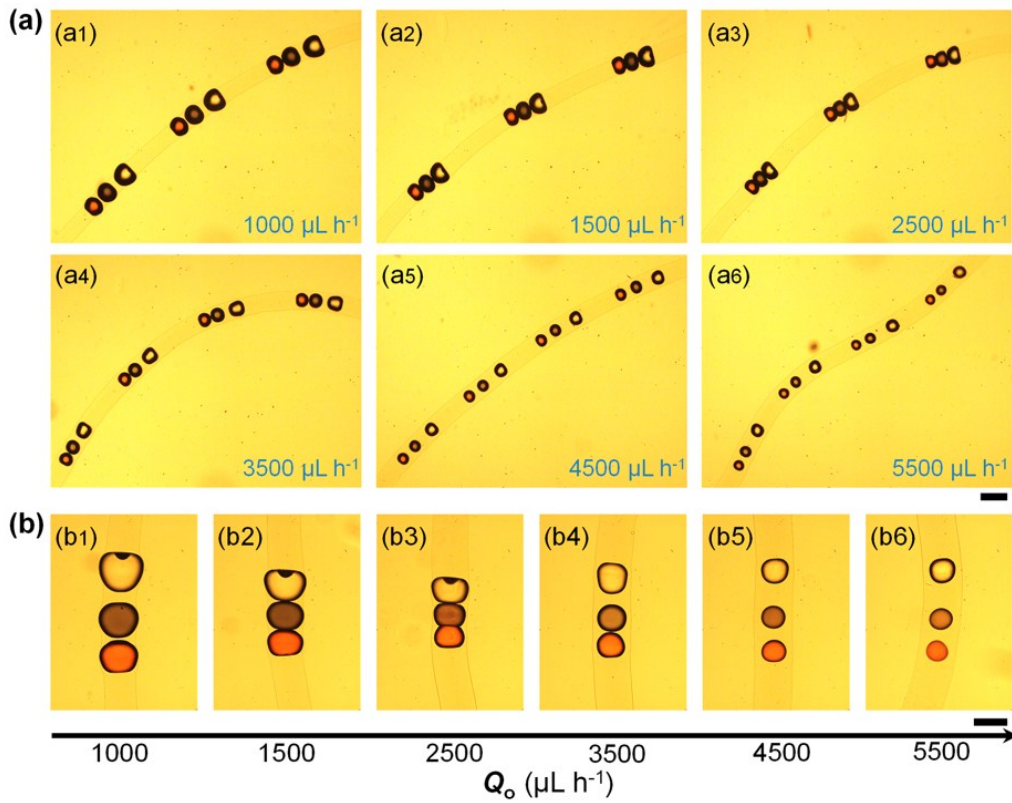
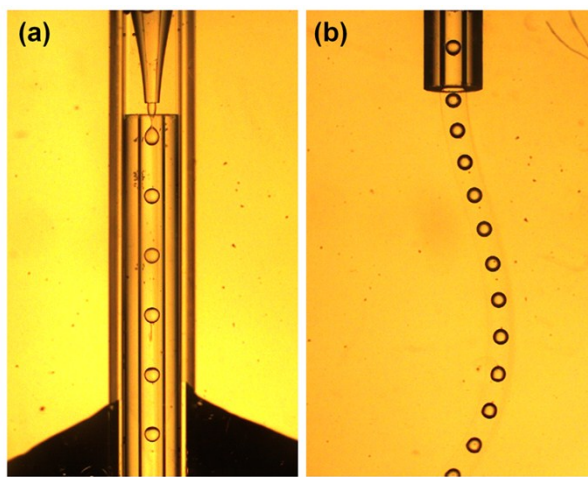


**Figure S8.** Microfluidic controllable generation of encoded microfibres with three different types of microdots. (a) Optical microscope images of microfibres with the encoding unit of different dye-filled microdots by changing the oil flow rate ( $Q_0$ ). The scale bar is 500  $\mu\text{m}$ . (b) Magnified optical microscope images of the encoded microfibres fabricated by different flow rate  $Q_0$ . The size of each microdot in microfibres decreases with the increasing of the flow rate  $Q_0$ . The scale bar is 300  $\mu\text{m}$ . The flow control of the alginate solution can help to create more space between each microdots to avoid the coalescence. In addition, reducing the length of the outlet tube may also help to create enough space between each microdot.

### Part III. Supplementary videos S1, S2 and S3

#### Video S1

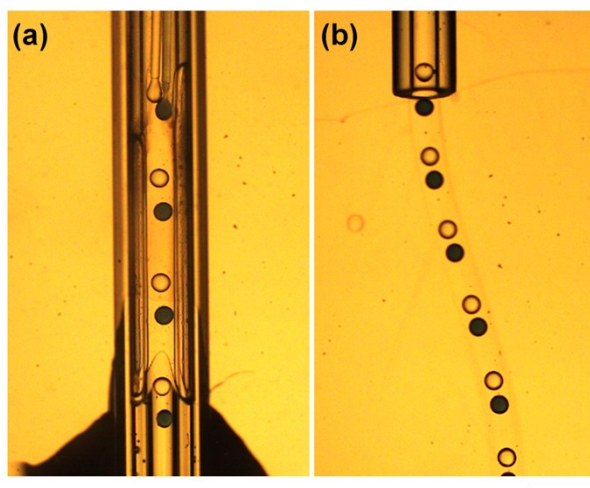
Microfluidic generation of encoded microfibre with one encoding element



Video shows the generation of one type of the droplet (a) and the microfibre solidification process (b). The flow rates of  $Q_i$  (no dye) and  $Q_o$  are at 300 and 2500  $\mu\text{L h}^{-1}$ , respectively. The scale bar is 1000  $\mu\text{m}$ .

#### Video S2

Microfluidic generation of encoded microfibre with two encoding elements



Video shows the generation of two types of the droplets (a) and the microfibre solidification process (b). The flow rates of  $Q_{i1}$  (no dye),  $Q_{i3}$  (black dye) and  $Q_o$  at 200, 200 and 3000  $\mu\text{L h}^{-1}$ , respectively. The scale bar is 1000  $\mu\text{m}$ .

